プリオンワクチン開発の大きな障害となっている。従って，プリオンワクチンの成功のカギは，いかに免疫寛容を破壊し，効率よく抗体を産生させることができるかにかかっている。

4.2 異種 PrP によるプリオンワクチン

我々はウシ及びヒツジの異種レコンビナント PrP が BALB/c マウスにおいて，わずかであるが，プリオンワクチンとして有意な効果を示したことを報告した[32]。非免疫の BALB/c マウスに福岡-1 プリオン株を腹腔内に感染させると，これらのマウスは感染後約 291 日前後で発症した（図 3 A)。マウスレコンビナント PrP を免疫しても，抗体産生はほとんど認められず，プリオン病の発症遅延も観察されなかった（図 3 A)。この結果は，マウスレコンビナント PrP がマウスにおいて免疫寛容であることと一致した。一方，ウシ及びヒツジレコンビナント PrP を免疫したマウスでは，特異抗体及びマウス PrP と反応する自己抗体の産生が認められた。また興

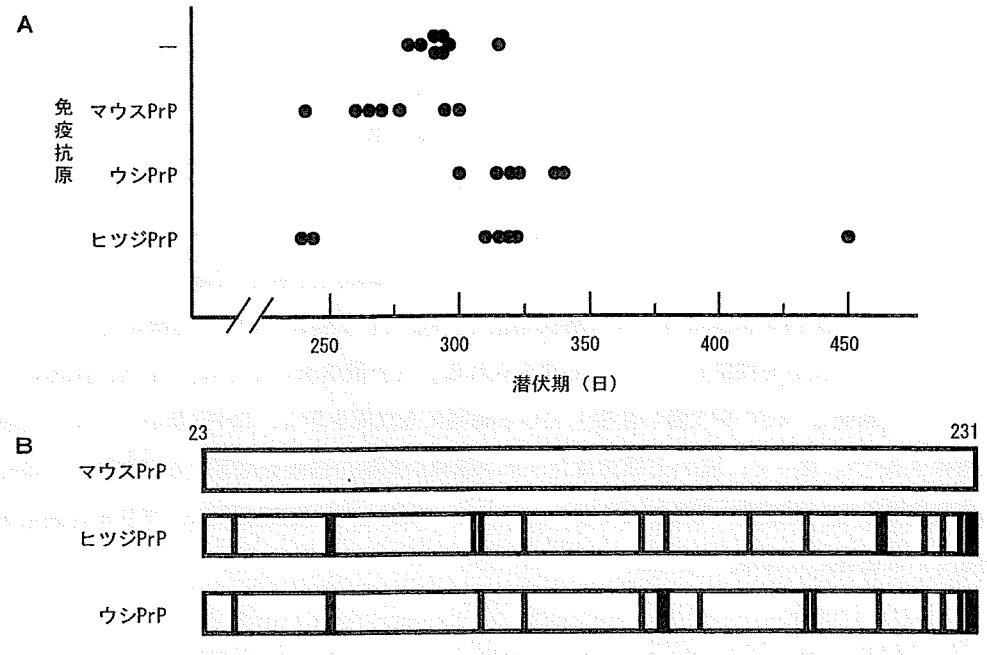

図 3

A：異種レコンビナント PrP 免疫によるワクチン効果。それぞれのレコンビナント PrP を BALB/c マウスの腹腔内に 2 週間おきに 5 回免疫した後，福岡-1 プリオンを腹腔内に感染させた。マウスレコンビナント PrP を免疫しても，非免疫マウスと比べて，プリオン病の発症遅延は観察されなかった。一方，ウシ及びヒツジ異種レコンビナント PrP を免疫されたマウスでは，プリオン病の発症遅延が認められた。

B：動物種間における PrP のアミノ酸の違い。ウシ及びヒツジ PrP はマウス PrP に高い相同性を示す。しかし，いくつかのアミノ酸はそれぞれの種により異なる。マウス PrP と異なるアミノ酸を棒線で表している。

味深いことに，ウシレコンビナントPrPを免疫したマウスは，プリオンを感染させると感染後322日前後でプリオン病を発症し，有意な発症遅延を示した（p=0.0008）（図3A）。また，ヒツジレコンビナントPrPを免疫したマウスの約70%（7匹中5匹）でも，プリオン病の発症遅延が認められた（図3A）。驚くことに，その中の1匹は450日程度経過してプリオン病を発症し，著明なワクチン効果が認められた（図3A）。

宿主蛋白質と類似したアミノ酸組成を持つ外来抗原は，その宿主蛋白質と反応する自己抗体を誘導する[33,34]。PrPは動物種間において非常に保存された分子である。アミノ酸レベルで90%以上の相同性を示す（図3B）。しかし，動物種によりアミノ酸組成がわずかに異なる（図3B）。従って，ウシやヒツジレコンビナントPrPが抗原類似性を介して自己抗体産生を誘導し，プリオン病に対してワクチン効果を発揮したのではないかと考えられる。従って，PrPの抗原類似性をさらに高めることにより，もっと効果的なプリオンワクチンの開発が可能となるかもしれない。

4.3　免疫モデュレーターを用いたプリオンワクチン

CpGオリゴヌクレオチドはToll-like受容体と結合し免疫反応を刺激する免疫モデュレーターである[35]。実際，CpGをPrPと同時に免疫すると，PrPに対する免疫寛容が部分的に破壊され自己抗体が産生されることが報告されている[36,37]。また興味深いことに，CpGを腹腔内にプリオン感染7日後から毎日20日まで繰り返し投与しただけで，プリオン感染を著明に抑制できることが報告された[38]。コントロールマウスにRMLプリオンを感染させると，マウスは感染後181日前後でプリオン病を発病した[38]。しかし，CpGを投与されたマウスは330日経過してもプリオン病の症状を呈しなかった[38]。これらの結果は，CpG投与による自然免疫の活性化がプリオン病の予防に効果的であることを示唆した。しかし後に，CpGの繰り返し投与は免疫反応に重要な濾胞樹状細胞（follicular dendritic cell；FDC）の減少をもたらすことが報告された[39]。FDCはプリオンが脳内に侵入するまでのプリオン増殖の主要な場である。従って，CpGの抗プリオン活性は繰り返し投与によりもたらされたFDCの抑制ためと考えられた。

DNAワクチンについても報告されている。PrPをライソソームに局在するようなシグナルを融合させた蛋白質のDNAをマウスの筋肉に接種すると，PrPに対する自己抗体が誘導され，またBSE1プリオンの感染に対し予防効果を示したことが報告された[40]。DNAワクチンを投与されたマウスは，コントロールマウスと比べて，プリオン病の発症が約73日遅れた[40]。一方，PrPだけを発現するDNAワクチンの投与では，抗体産生は認められなかった[40]。従って，効果的なDNAワクチンを開発するためには，PrPの効果的な修飾が必要であることが示唆された。

4.4 PrPの修飾によるプリオンワクチン

Gilchらは，マウスPrPをタンデムにつないだダイマーPrPがC57BL/6マウスにおいて高い抗原性を有し，PrPに対する自己抗体を誘導することを報告した[41]。しかし後に他のグループにより，このダイマーPrPは確かに自己抗体を誘導するが，RMLプリオンの感染に対してワクチン効果を示さないことが報告された[42]。つまり，ダイマーPrPにより誘導された自己抗体は中和抗体として機能しない可能性が考えられた。

熱ショック蛋白質は強力な免疫アジュバント分子である。実際，熱ショック蛋白質の一つであるDnaKをPrPと融合させた蛋白質をBALB/cマウスに免疫すると，PrPに対する自己抗体が産生されることが報告された[43]。また，ウイルスのカプシド蛋白質は集合しウイルス様粒子（virus-like particle；VLP）を形成する。VLPは免疫反応を強く刺激する。Niklesらは，マウス白血病レトロウイルスのVLPの表面にPrPのC末領域を発現するレコンビナントVLPを作成しマウスに免疫したところ，PrPに対する自己抗体が産生されることを報告した[44]。また別のグループは，マウスPrP由来の9個のアミノ酸からなるペプチド（DWEDRYYRE）をウシパピローマウイルス-1VLPに発現させたところ，同様に自己抗体が産生されることを報告した[45]。これらの結果は，PrPを効果的に修飾することにより，PrPに対する免疫寛容を効果的に破壊できることを示した。しかし残念ながら，これらのワクチンがプリオン感染に効果的であるのか，動物を用いた実験データがない。

5 プリオン粘膜ワクチン

5.1 粘膜ワクチンの利点

これまでの通常のワクチンは注射針を用いて体内に接種するものである。このため，接種時に痛みを伴い，注射針やその他の器具の費用がかかる。また，ワクチン接種には熟練を要する。一方，粘膜ワクチンは鼻腔や気道の粘膜に噴霧するだけでよく，接種時の痛みもなく，注射針等の費用もかからない。また，熟練者もいらない。このように，粘膜ワクチンはこれまでのワクチンと比べて，多くの利点を有する[46]。さらに，粘膜ワクチンは免疫学的にもこれまでのワクチンに勝っている。これまでのワクチンはIgGを誘導するだけである。しかし，粘膜ワクチンはIgGのみでなくIgAも誘導できる。IgAはインフルエンザウイルスなどの粘膜を介した感染の予防に効果的である。従って，粘膜ワクチンは非粘膜及び粘膜を介した感染の予防に効果的である[46]。

5.2 細菌性トキシンを用いたプリオン粘膜ワクチン

コレラトキシン（CT）や大腸菌の易熱性エンテロトキシン（LT）は強力な粘膜アジュバント

である[47,48]。両者は，同じような構造を持ち，毒素活性を担う1分子のAサブユニットと細胞表面レセプター（GM1ガングリオシド）への結合に関与する5分子のBサブユニットから構成されている。Aサブユニットは毒性に関与するADPリボシルトランスフェラーゼ活性を有している。細胞表面のレセプターに結合することが粘膜アジュバント活性に必要であるが，詳細なメカニズムは不明である。

Badeらは，マウスレコンビナントPrP 90-231をCTと共にBALB/cマウスの鼻腔に投与すると，PrPに対する特異IgGとIgAが産生され，139Aプリオン感染にわずかであるが有意なワクチン効果を示したことを報告した[49]。コントロールマウスは感染後258日前後でプリオン病を発症したのに対し，免疫マウスは266日に発症した[49]。

我々は，LTのBサブユニット（LTB）をマウスレコンビナントPrP 120-231及びウシレコンビナントPrP 132-242に融合させた蛋白質を作成し，それぞれの粘膜抗原性をBALB/cマウスの鼻腔内に投与し調べた（図4A）[50]。非融合マウスレコンビナントPrP 120-231は免疫寛容のため抗体産生を誘導しなかった（図4B）[50]。しかし，LTBと融合させると，マウスレコンビナントPrP 120-231の抗原性が上昇し，わずかであるが有意な抗体産生を示した（図4B）[50]。また，ウシレコンビナントPrP 132-242のみでも中程度のIgG産生が誘導されたが，LTBと融合することにより，より多くのIgG及びIgA産生が誘導された（図4B）[50]。しかし，マウスPrPと反応する自己抗体の量は低かった[50]。

5.3　サルモネラ菌をベクターとするプリオン粘膜ワクチン

乳酸桿菌やサルモネラ菌などの腸管に共生する細菌が粘膜免疫のベクターとして有用であることが明らかとなってきている[51]。Goñiらは，弱毒ワクチン株であるネズミチフス菌（*Salmonella typhimurium* LVR 01 LPS）にマウスPrPと破傷風トキシンの非毒性フラグメントCとの融合蛋白を発現させ，CD-1マウスに経口的に投与した[52]。その結果，PrPに特異的に反応するIgG及びIgAの産生を認めた[52]。また興味深いことに，これらのマウスに139Aプリオンを経口的に感染した結果，約30%のマウスで著明な潜伏期の延長が認められ，500日経過してもプリオン病特異的な症状が認められなかった[52]。この潜伏期の延長は産生された抗PrP抗体の力価と非常に相関した[53]。一方，コントロールマウスはプリオン感染後300日内に全て死亡した[52]。

ワクチン株であるLVR 01 LPSネズミチフス菌は腸管に共生する。従って，PrPは腸管内で長期間そして大量に産生されると考えられる。このように大量のPrPが長期間腸管内に存在することにより，粘膜免疫が刺激されたのではないかと考えられる。また，フラグメントCは高い抗原性を有する。従って，フラグメントCと融合することにより，PrPの粘膜抗原性が増強された可能性も考えられる。しかし，残りの70%のマウスでは，ワクチン効果はわずかである

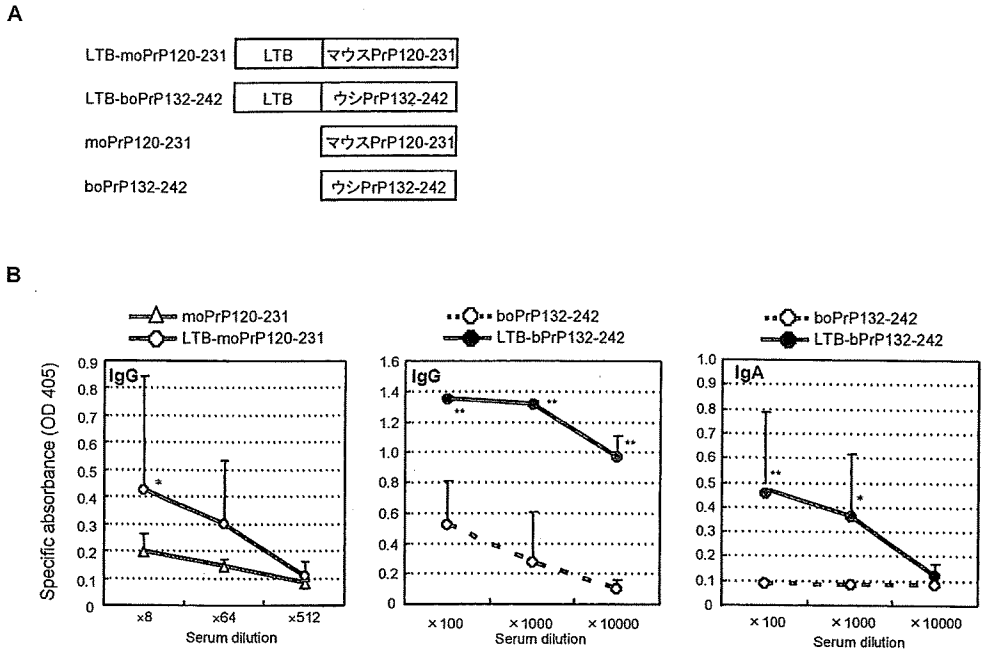

図 4

A：LTB 融合及び非融合 PrP の構造。C 末の半分の領域に相当するマウス PrP 120-231 とウシ PrP 132-242 を LTB と融合させた。

B：LTB 融合によるマウス及びウシ PrP の粘膜抗原性の増強。LTB 融合マウス及びウシ PrP を BALB/c マウスの鼻腔内に 2 週間おきに 3 回投与し，血清 IgG 及び IgG の産生を調べた。LTB 非融合マウス PrP 120-231 では抗体産生が認められなかったが，LTB 融合マウス PrP 120-231 では有意に増加した抗体産生が認められた。また，同様に，LTB を融合したウシ PrP 132-242 の方が非融合ウシ PrP 132-242 よりも明らかに粘膜抗原性が高く，より高い力価の IgG 及び IgA の産生を誘導した。

か，またはほとんど認められなかった。従って，免疫した個体の全てにいかに効率よく高力価の抗体産生を誘導することができるかが，このワクチンの今後の課題である。

6　プリオンワクチンの問題点と今後の展開

PrP^c は宿主蛋白質である。従って，PrP^c と反応する抗体を誘導するワクチンは，自己免疫反応を誘発するかもしれない。マウスにおいては，関節の腫脹や異常行動等の異常所見は報告されていない。しかし，ヒトではどのようなことが起こるのか予測できない。宿主蛋白質であるアミロイド前駆蛋白質由来の Aβ ペプチドを用いたアルツハイマー病ワクチンでも，マウスでは何ら副作用は報告されていない[54,55]。しかし，ヒトに投与すると，一部のヒトに脳炎の重篤な副作

用が起こることが報告された[54,55]。従って，PrP^C をターゲットとしたワクチンよりも，PrP^{Sc} をターゲットとしたワクチン開発の方が望ましいのかもしれない。

PrP^C と PrP^{Sc} は蛋白質構造が異なる。Cashman らのグループはこのことを利用して，PrP^C では蛋白質内部に埋もれているけれど，PrP^{Sc} では外部に露出していると考えられる部位を同定し，その部分のペプチドをマウス等の実験動物に免疫して，PrP^{Sc} に特異的な抗体が産生されるのか検討した[56]。興味深いことに，彼らの期待した通りに，免疫した動物からは PrP^{Sc} 特異的に反応する抗体が得られた[56]。しかし，このようなワクチンがプリオン病に効果があるのか，動物を用いた実験を行う必要がある。

通常のウイルス感染と同様に，プリオン感染においても干渉という現象が存在する[57,58]。二つの異なるプリオン株を感染させると，一つのプリオンが他のプリオンの感染を阻害する。ウイルス感染の場合は，インターフェロンが重要な役割を担っている。しかし，プリオンの場合には，あまり関与していないと考えられている。このプリオン干渉の分子メカニズムを解明することは，新規のプリオンワクチンの開発に繋がる可能性を秘めている。

文　　献

1） S. B. Prusiner, *Biochemistry*, **31**, 12277-12288 (1992)
2） S. J. DeArmond, *et al., Am. J. Pathol.*, **146**, 785-811 (1995)
3） S. B. Prusiner, *Proc. Natl. Acad. Sci. USA*, **95**, 13363-13383 (1998)
4） M. Noguchi-Shinohara *et al., Nippon rinsho*, **65**, 1379-1383 (2007)
5） J. P. Brandel *et al., Lancet*, **362**, 128-130 (2003)
6） L. Cervenakova *et al., Proc. Natl. Acad. Sci. USA*, **95**, 13239-13241 (1998)
7） C. A. Llewelyn *et al., Lancet*, **363**, 417-421 (2004)
8） A. H. Peden *et al., Lancet*, **364**, 527-529 (2004)
9） S. J. Wroe *et al., Lancet*, **368**, 2061-2067 (2006)
10） E. S. Williams. *Vet. Pathol.*, **42**, 530-549 (2005)
11） S. B. Prusiner, *Science*, **216**, 136-144 (1982)
12） N. Stahl *et al., Cell*, **51**, 229-240 (1987)
13） J. Collinge *et al., Nature*, **370**, 295-297 (1994)
14） I. Tobler *et al., Nature*, **380**, 639-642 (1996)
15） Y. Sakurai-Yamashita *et al., Neuroscience*, **136**, 281-287 (2005)
16） N. F. McLennan *et al., Am. J. Pathol.*, **165**, 227-235 (2004)
17） N. Nishida *et al., Lab. Invest.*, **79**, 689-697 (1999)
18） K. M. Pan *et al., Proc. Natl. Acad. Sci. USA*, **90**, 10962-10966 (1993)
19） F. E. Cohen *et al., Science*, **264**, 530-531 (1994)

20) P. T. Lansbury, *Science*, **265**, 1510 (1994)
21) H. Bueler *et al.*, *Cell*, **73**, 1339-1347 (1993)
22) S. B. Prusiner *et al.*, *Proc. Natl. Acad. Sci. USA*, **90**, 10608-10612 (1993)
23) J. C. Manson *et al.*, *Neurodegeneration*, **3**, 331-340 (1994)
24) S. Sakaguchi *et al.*, *Journal of virology*, **69**, 7586-7592 (1995)
25) B. Chesebro *et al.*, *Science*, **308**, 1435-1439 (2005)
26) A. R. White *et al.*, *Nature*, **422**, 80-83 (2003)
27) K. Kaneko *et al.*, *Proc. Natl. Acad. Sci. USA*, **92**, 11160-11164 (1995)
28) M. Horiuchi *et al.*, *The EMBO journal*, **18**, 3193-3203 (1999)
29) V. Perrier *et al.*, *J. Neurochem.*, **89**, 454-463 (2004)
30) D. Peretz *et al.*, *Nature*, **412**, 739-743 (2001)
31) M. Enari *et al.*, *Proc. Natl. Acad. Sci. USA*, **98**, 9295-9299 (2001)
32) D. Ishibashi *et al.*, *Vaccine*, **25**, 985-992 (2007)
33) S. M. Behar *et al.*, *Arthritis and rheumatism*, **38**, 458-476 (1995)
34) C. W. Ang *et al.*, *Trends in immunology*, **25**, 61-66 (2004)
35) D. T. O'Hagan *et al.*, *Biomolecular engineering*, **18**, 69-85 (2001)
36) M. B. Rosset *et al.*, *J. Immunol*, **172**, 5168-5174 (2004)
37) D. S. Spinner *et al.*, *Journal of leukocyte biology.*, **81**, 1374-1385 (2007)
38) S. Sethi *et al.*, *Lancet*, **360**, 229-230 (2002)
39) M. Heikenwalder *et al.*, *Nature medicine*, **10**, 187-192 (2004)
40) N. Fernandez-Borges *et al.*, *Journal of virology*, **80**, 9970-9976 (2006)
41) S. Gilch *et al.*, *The Journal of biological chemistry*, **278**, 18524-18531 (2003)
42) M. Polymenidou *et al.*, *Proc. Natl. Acad. Sci. USA*, **101**, 14670-14676 (2004)
43) M. F. Koller *et al.*, *J. Neuroimmunol*, **132**, 113-116 (2002)
44) D. Nikles *et al.*, *Journal of virology*, **79**, 4033-4042 (2005)
45) A. Handisurya *et al.*, *Febs. J.*, **274**, 1747-1758 (2007)
46) E. L. Giudice *et al.*, *Advanced drug delivery reviews*, **58**, 68-89 (2006)
47) T. O. Nashar *et al.*, *Vaccine*, **11**, 235-240 (1993)
48) J. Holmgren *et al.*, *Vaccine*, **21**, S 89-95 (2003)
49) S. Bade *et al.*, *Vaccine*, **24**, 1242-1253 (2006)
50) H. Yamanaka *et al.*, *Vaccine*, **24**, 2815-2823 (2006)
51) M. T. De Magistris, *Advanced drug delivery reviews*, **58**, 52-67 (2006)
52) F. Goni *et al.*, *Neuroscience*, **133**, 413-421 (2005)
53) F. Goni *et al.*, *Neuroscience*, **153**, 679-686 (2008)
54) D. S. Gelinas *et al.*, *Proc. Natl. Acad. Sci. USA*, **101**, 14657-14662 (2004)
55) D. Schenk *et al.*, *Current opinion in immunology*, **16**, 599-606 (2004)
56) E. Paramithiotis *et al.*, *Nature medicine*, **9**, 893-899 (2003)
57) L. Manuelidis, *Proc. Natl. Acad. Sci. USA*, **95**, 2520-2525 (1998)
58) N. Nishida *et al.*, *Science*, **310**, 493-496 (2005)

the FEBS Journal

Hyperefficient PrP^{Sc} amplification of mouse-adapted BSE and scrapie strain by protein misfolding cyclic amplification technique

Aiko Fujihara, Ryuichiro Atarashi, Takayuki Fuse, Kaori Ubagai, Takehiro Nakagaki, Naohiro Yamaguchi, Daisuke Ishibashi, Shigeru Katamine and Noriyuki Nishida

Department of Molecular Microbiology and Immunology, Nagasaki University Graduate School of Biomedical Sciences, Japan

Keywords
prion; protein misfolding cyclic amplification; sonication; transmissible spongiform encephalopathy

Correspondence
R. Atarashi, Department of Molecular Microbiology and Immunology, Nagasaki University Graduate School of Biomedical Sciences, 1-12-4 Sakamoto, Nagasaki 852-8523, Japan
Fax: +81 95 819 7060
Tel: +81 95 819 7060
E-mail: atarashi@nagasaki-u.ac.jp

(Received 19 February 2009, revised 11 March 2009, accepted 16 March 2009)

doi:10.1111/j.1742-4658.2009.07007.x

Abnormal forms of prion protein (PrP^{Sc}) accumulate via structural conversion of normal PrP (PrP^{C}) in the progression of transmissible spongiform encephalopathy. Under cell-free conditions, the process can be efficiently replicated using *in vitro* PrP^{Sc} amplification methods, including protein misfolding cyclic amplification. These methods enable ultrasensitive detection of PrP^{Sc}; however, there remain difficulties in utilizing them in practice. For example, to date, several rounds of protein misfolding cyclic amplification have been necessary to reach maximal sensitivity, which not only take several weeks, but also result in an increased risk of contamination. In this study, we sought to further promote the rate of PrP^{Sc} amplification in the protein misfolding cyclic amplification technique using mouse transmissible spongiform encephalopathy models infected with either mouse-adapted bovine spongiform encephalopathy or mouse-adapted scrapie, Chandler strain. Here, we demonstrate that appropriate regulation of sonication dramatically accelerates PrP^{Sc} amplification in both strains. In fact, we reached maximum sensitivity, allowing the ultrasensitive detection of < 1 LD_{50} of PrP^{Sc} in the diluted brain homogenates, after only one or two reaction rounds, and in addition, we detected PrP^{Sc} in the plasma of mouse-adapted bovine spongiform encephalopathy-infected mice. We believe that these results will advance the establishment of a fast, ultrasensitive diagnostic test for transmissible spongiform encephalopathies.

Transmissible spongiform encephalopathies (TSEs), or prion diseases, are a series of fatal neurodegenerative diseases that include Creutzfeldt–Jakob disease (CJD) in humans, scrapie in sheep and bovine spongiform encephalopathy (BSE) in cattle. In the late 1990s, contamination of the human food chain by BSE-infected cattle caused variant CJD (vCJD), mainly in the UK [1,2]. Moreover, it has been reported that vCJD may be transmitted by blood transfusion [3], probably because the species barrier between cattle and humans is markedly diminished at secondary transmission. Hence, a blood screening test is urgently needed to prevent the spread of vCJD infection. In addition, early diagnosis is required to provide the opportunity for treatment of TSEs.

The key molecular event in the progression of TSEs is the continuous conformational conversion of the normal cellular form of prion protein (PrP^{C}) to the abnormal isoform (PrP^{Sc}). According to the seeding model hypothesis for prion propagation, PrP^{C} converts

Abbreviations
BH, brain homogenate; BSE, bovine spongiform encephalopathy; CJD, Creutzfeldt–Jakob disease; mBSE, mouse-adapted BSE; NBH, normal brain homogenate; PK, proteinase K; PMCA, protein misfolding cyclic amplification; PNGase F, peptide: N-glycosidase F; PrP^{C}, normal cellular form of PrP; PrP^{Sc}, abnormal forms of prion protein; rMoPrP, recombinant mouse PrP; TSE, transmissible spongiform encephalopathy; vCJD, variant CJD.

to PrP^{Sc} only at the end of PrP^{Sc} polymers [4], indicating that the PrP^{Sc} accumulation rate is regulated by the number of polymers. An increase in the number of PrP^{Sc} polymers is acquired mainly by breaking large PrP^{Sc} polymers into smaller units. Although the *in vivo* factor remains unknown, the use of sonication to mimic the fragmentation process has been successfully applied in the development of an *in vitro* PrP^{Sc} amplification technique, designated protein misfolding cyclic amplification (PMCA) [5]. Using this technique, ultrasensitive PrP^{Sc} detection in easily accessible specimens such as blood and urine was first achieved in a hamster model infected with hamster-adapted scrapie, 263K strain [6–8]. The results suggest that PMCA is one of the most promising approaches for the development of a blood screening test and the early diagnosis of TSEs. However, a number of PMCA rounds are needed to reach maximal sensitivity [9], which not only takes several weeks, but also results in an increased risk of contamination. Furthermore, although mild amplification has also been demonstrated in other mammalian species, such as mice, cervids and humans, the amplification levels in these species are lower than those in hamster [10–13]. More recently, the addition of a synthetic polyanion, polyadenylic acid, was found to enhance PrP^{Sc} amplification in the PMCA, but spontaneous PrP^{Sc} formation was observed after several reaction rounds, which may make it difficult to detect genuine PrP^{Sc} in specimens [14,15]. The use of recombinant PrP as the amplification substrate enabled faster and simpler detection than conventional PMCA methods using brain homogenate [16–20], but attempts to use blood from TSEs-infected animals as a seed for the amplification assay have not yet been successful. Thus, further studies are required to establish these amplification methods as practical diagnostic assays.

The aim of this study was to find the conditions that promote PrP^{Sc} amplification using the PMCA technique. We chose mouse-adapted BSE (mBSE) and mouse-adapted scrapie, Chandler strain, as animal models for TSEs. Here, we describe a hyperefficient amplification of PrP^{Sc} in the two strains, which was achieved by modulating the sonication conditions.

Results and Discussion

Effect of EDTA and digitonin on PMCA

Prior to starting PMCA, we confirmed the presence of PrP^{Sc} in mBSE-brain homogenate (BH) and Chandler-BH by western blot analysis. PrP^{Sc} accumulation was detected with mouse anti-(PrP ICSM35) mAb in both mBSE-BH and Chandler-BH, whereas none was

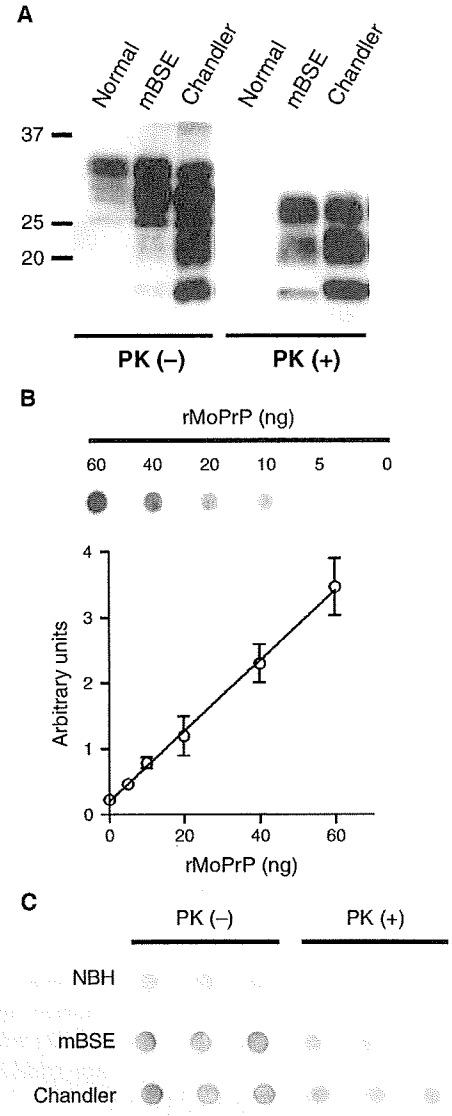

Fig. 1. Estimation of PrP^{Sc} concentration in mBSE-BH and Chandler-BH by dot-blot analysis. (A) Detection of PrP in NBH, mBSE-BH and Chandler-BH without (–) or with (+) PK treatment using western blots with anti-PrP mAb ICSM35. Each lane contains 50 μg total protein. (B) The designated amounts of recombinant mouse PrP (rMoPrP) were used as standards for the dot-blot analysis. Linear regression between dot intensities (arbitrary units) and rMoPrP is shown ($n = 3$, average ± SD, $r^2 = 0.967$). (C) NBH, mBSE-BH and Chandler-BH without (–) or with (+) PK treatment (40 $\mu g \cdot mL^{-1}$ at 37 °C for 1 h) were analyzed ($n = 3$). All three panels were obtained from the same membrane. The regression line in (B) represents the concentrations of PrP^{Sc}.

detected in normal BH (Fig. 1A). The PrP^{Sc} concentrations in these BHs were estimated by dot-blotting analysis using recombinant mouse PrP as standard (Fig. 1B,C). The average PrP^{Sc} concentrations in

mBSE-BH and Chandler-BH were 1.21 and 1.86 $\mu g \cdot mg^{-1}$ of total protein, respectively.

When conventional PMCA is performed on BHs, EDTA is usually added to the reaction mixture [9]. In addition, imidazole has been reported to stimulate PrP^{Sc} amplification in PMCA using PrP^{C} purified from normal BH (NBH) as the substrate [21]. Divalent metal ions, in particular copper and zinc, are known to inhibit conversion to PrP^{Sc} [21] and fibril formation in recombinant PrP [22], and EDTA and imidazole are presumed to minimize the inhibitory action of metal ions. Accordingly, we conducted PMCA with or without these chemicals to examine the effect on amplification. As shown in Fig. 2A, 1–10 mM EDTA was needed for the efficient amplification of Chandler-PrP^{Sc}, whereas 10–100 mM imidazole had little effect. Similar results were obtained for mBSE-PrP^{Sc} (data not shown). It is possible that many impurities in crude BH interfere with the action of imidazole, which binds weakly to divalent metal ions, but do not interfere with the action of EDTA, a powerful chelating agent.

We tested the effect of digitonin on the PMCA reaction, because it has been shown that proteinase K (PK)-resistant PrP fragments form in mouse NBH, and this formation is inhibited by the presence of 0.05% digitonin [11]. We observed that PK-resistant PrP bands in NBH were clearly detected by SAF83 antibody, which has an epitope located within PrP residues 126–164, but hardly detected by ICSM35, the epitope of which is located at residues 92–101 (Fig. 2B). By contrast, both antibodies recognized mBSE-PrP^{Sc} amplified by PMCA (Fig. 2B). The main fragment of the PK-resistant PrP in NBH, designated $PrPres^{(NBH)}$, was ~25 kDa, i.e. smaller than the 27 kDa fragment typical of diglycosylated PrP^{Sc}. Following serial treatment with PK and peptide:N-glycosidase F (PNGase F), a single 16 kDa band of nonglycosylated $PrPres^{(NBH)}$ was detected; the fragments of nonglycosylated mBSE- and Chandler-PrP^{Sc} were estimated to be 17 and 18 kDa, respectively (Fig. 2C). The results indicate that the PK-cleavage point of $PrPres^{(NBH)}$ is positioned closer to the C-terminus than the PK-cleavage point of PrP^{Sc}. Moreover, the amount of $PrPres^{(NBH)}$ could be decreased by repeating the sonication, particularly in the presence of 0.05% digitonin (Fig. 2B). By contrast, the amplification and final quantity of PrP^{Sc} were not affected by digitonin (Fig. 2B,C), indicating that $PrPres^{(NBH)}$ does not interfere with PrP^{Sc} amplification and is quite distinct from the spontaneous formation of PrP^{Sc} reported previously [14,15]. We also found that formation of $PrPres^{(NBH)}$ was promoted by the presence of EDTA and detergent (A. Fujihara and R. Atarashi, unpublished data).

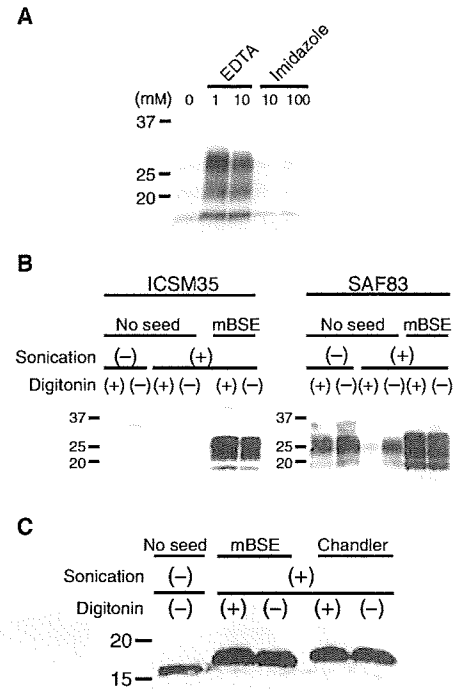

Fig. 2. The effects of EDTA and digitonin on PMCA reactions. (A) The effect of the indicated concentrations of EDTA and imidazole on the PMCA reactions using diluted Chandler-BH containing 1 ng PrP^{Sc} as seeds. Sonication was performed over 24 h with 40-s pulses every 30 min at 60% power. Samples were digested with PK and probed with ICSM35. (B) The effect of 0.05% digitonin on the PMCA reactions and the formation of PK-resistant PrP in NBH ($PrPres^{(NBH)}$). No seed, reaction mixtures containing only NBH were incubated for 24 h, without (–) or with (+) periodic sonication. mBSE, PMCA with (+) or without (–) digitonin was carried out using diluted mBSE-BH containing 1 ng of PrP^{Sc} as seeds. Sonication was performed as in (B). PK-treated samples were analyzed by western blotting with ICSM35 (epitope located at mouse PrP amino acids 92–101) or SAF83 (epitope located within amino acids 126–164). (C) Size differences between $PrPres^{(NBH)}$ and mBSE- and Chandler-PrP^{Sc} amplified by PMCA with (+) or without (–) digitonin after consecutive treatments with PK and PNGase F. Samples were probed with SAF83. Molecular mass markers are indicated in kDa on the left.

Of note, small amounts of detergent-insoluble and PK-resistant PrP aggregates have been reported in uninfected human brains in the presence of EDTA and detergent [23]. However, the exact mechanism by which these PK-resistant PrP conformers are generated in NBH remains to be determined. Digitonin does not appear to enhance the amplification of PrP^{Sc}, but it does help clarify the PMCA results, especially when an antibody that recognizes the C-terminal part of PrP is used. After reviewing the results shown in Fig. 2, we decided to add 1 mM EDTA and 0.05% digitonin to the reaction mixture in subsequent experiments.

The influence of sonication times on the rate of PMCA

To investigate how sonication conditions influence the PrP^{Sc} amplification rate, we carried out PMCA at various sonication times (5, 10, 20, 40 and 60 s) per cycle, using serially diluted mBSE- or Chandler-BH containing any one of 1 ng (10^{-9} g), 10 pg (10^{-11} g), 100 fg (10^{-13} g) or 1 fg (10^{-15} g) of PrP^{Sc} as seeds for the reaction. Surprisingly, the rate of PrP^{Sc} amplification varied dramatically according to the sonication time (Fig. 3A,B), peaking at 10 s sonication for mBSE and 20 s for Chandler, every 30 min. Under these conditions, all dilutions of mBSE- or Chandler-BH (from 1 ng to 1 fg PrP^{Sc}) were readily detectable in a single reaction round (96 cycles, 48 h) (Fig. 3A,B). The results were reproduced in three independent experiments (data not shown). To determine the minimum amount of PrP^{Sc} detectable by PMCA under optimal conditions, further dilutions of mBSE-BH and Chandler-BH to 1–10 ag (10^{-18} to 10^{-17} g) of PrP^{Sc} were tested. When seeded with mBSE-BH, two of four replicates with 10 ag PrP^{Sc} and three of four replicates with 1 ag PrP^{Sc} were detected after one 48 h reaction round (Fig. 3C). With Chandler-BH, however, only one of four replicates with 10 ag PrP^{Sc}

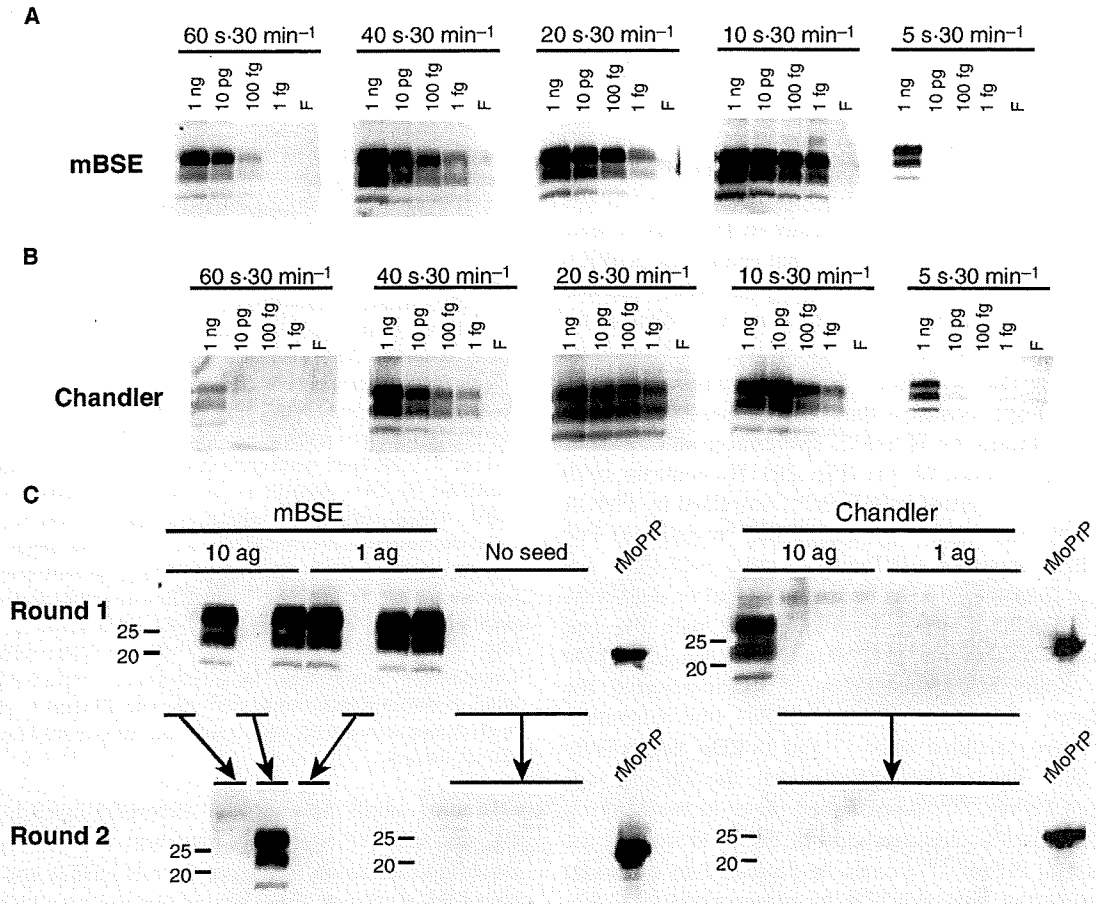

Fig. 3. Influence of sonication time on the rate of PrP^{Sc} amplification. PMCA was performed at various sonication times (5, 10, 20, 40 and 60 s) every 30 min at 60% power for 48 h using serially diluted mBSE-BH (A) or Chandler-BH (B) containing the designated amount of PrP^{Sc} as seeds. For reference, 1 ng PrP^{Sc} of mBSE and Chandler correspond to 4.7×10^{-4} and 6.5×10^{-4} dilution of infected BHs, respectively. F, frozen control containing 1 ng PrP^{Sc}. (C) PMCA was performed with a 10-s sonication pulse for mBSE and a 20-s pulse for Chandler every 30 min for 48 h. Round 1, first-round of PMCA using serially diluted mBSE-BH or Chandler-BH containing 1 or 10 ag PrP^{Sc} as seeds. No seed, the same volume of PMCA buffer was added to the reaction mixture as a negative control. All reactions were performed in quadruplicate. Round 2, 10% of each first round reaction volume (8 μL) was used to seed a second round of PMCA. All samples were digested with PK and analyzed by western blotting with ICSM35.

and none of the replicates with 1 ag PrP^{Sc} was detected (Fig. 3C). After a second serial PMCA reaction, another of the two replicates with 10 ag PrP^{Sc} of mBSE-BH, which were negative in the first round, became positive; the other remained negative (Fig. 3C). Moreover, further rounds did not increase the sensitivity of PrP^{Sc} detection (data not shown). None of the negative controls (no seed) produced detectable PrP^{Sc} bands after a second round of reactions (Fig. 3C), or after third and fourth rounds (data not shown), indicating that there was no spontaneous formation of PrP^{Sc} in our PMCA reactions. Although the PMCA experiments were performed very carefully to obtain consistent data, some discrepancies existed in the results shown in Fig. 3C (two of four for 10 ag PrP^{Sc} versus three of four for 1 ag PrP^{Sc} in the first round seeded with mBSE-BH, etc.), which may have resulted from positional influence on the delivery of vibrational energy to the samples when very low amounts (1–10 ag) of PrP^{Sc} were used as seeds. Nonetheless, these results provide evidence that the one 48 h reaction round almost reached maximum sensitivity. The efficiencies of PrP^{Sc} amplification in this study were greatly improved compared with previous studies using Chandler strain, which detected PrP^{Sc} in only 10^{-3} to 10^{-4}-diluted infected BHs after one round of PMCA [10,11]. Indeed, we were consistently able to detect 1 fg of PrP^{Sc} (6.5×10^{-10} dilution of Chandler-BHs). Thus, the increased amplification rate was at least $> 10^6$-fold (Table 1). We believe that this increased amplification rate will contribute to reducing the time required for ultrasensitive detection, and also minimize the risk of contamination.

The approximately 10-fold difference in the sensitivity between mBSE and Chandler may be caused by differences between the minimum size of PrP^{Sc} polymers that can act as seeds for PMCA reactions. Filtration studies have shown that type 1 and type 2 human PrP^{Sc} have different-sized aggregates [24]. Moreover, it is noteworthy that the quantity of PrP^{Sc} per unit of intracerebral LD_{50} in mBSE-BH was 7.5-fold less than that in Chandler-BH (4 versus 30 fg PrP^{Sc}), according to our end-point dilution bioassays. These findings may reflect differences in the size distribution of PrP^{Sc} between the two strains.

Fragmentation of PrP^{Sc} polymers by sonication is generally considered to lead to an increase in the number of PrP^{Sc} polymers, resulting in enhanced amplification [5]. However, at the same time, sonication may partially disrupt the PrP^{Sc} aggregate, so that the amplification rate is suppressed, in proportion to the disruption. In keeping with this assumption, it has been reported that the infectious titer of sonicated Chandler-BH is significantly decreased [25]. In addition, studies using flow field-fractionation revealed that the infectivity and converting activity of PrP^{Sc} purified from 263K-infected hamster brains peaked in oligomers consisting of 14–28 PrP molecules, whereas both activities were substantially absent in oligomers of < 5 PrP molecules [26]. Therefore, hyperefficient amplification of PrP^{Sc} appears to be achieved by an appropriate balance between the two opposing effects of sonication on the amplification of PrP^{Sc}.

Ultrasensitive detection of PrP^{Sc} in plasma from mBSE-infected mice

Because plasma is one of the most accessible specimens, and presumably contains only a very small amount of PrP^{Sc}, we collected plasma samples from four mBSE-infected mice showing clinical signs of TSEs and four uninfected control animals, and performed PMCA to compare seeding activity. In the control reactions, no PrP^{Sc} was seen in the first and second rounds (Fig. 4, lanes 5–8). By contrast, after only one reaction round seeded with mBSE plasma, two of four samples generated clear PrP^{Sc} bands (Fig. 3A, lanes 1 and 2) and a further sample exhibited less distinct bands (Fig. 4A, lane 3). After the second-round reactions, three samples produced strong PrP^{Sc} bands (Fig. 4B, lanes 1–3), but the remaining sample lacked PrP^{Sc} (Fig. 4B, lane 4), and further rounds did not improve the sensitivity (data not shown). The exact reason for the existence of the one negative sample seeded with mBSE-plasma is uncertain, but it is possible that there may be variation in the amount of PrP^{Sc}

Table 1. Comparison of the sensitivity of one-round PMCA to detect Chandler-PrP^{Sc} with the results of previous studies.

Sensitivity[a]	Sonicator	Sonication conditions	References
6.5×10^{-10}	Misonix, Model 3000	20 s every 30 min at 60% power	This study
2.0×10^{-3}	Bandelin Electronic, Model Sonopuls	Five pulses of 0.1 s at 0.9-s intervals every hour at 40% power	10
1.0×10^{-4}	Elekon, ELESTEIN 070-GOT	Five pulses of 3 s at 1-s interval every 30 min	11

[a] Sensitivity is shown as a dilution of Chandler-infected BH.

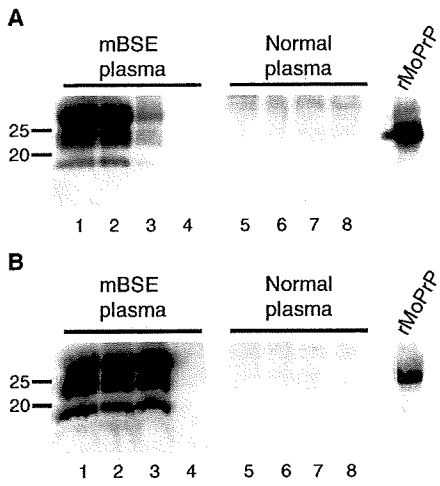

Fig. 4. Amplification of PrP^{Sc} in plasma of mBSE-infected mice by PMCA. (A) Aliquots (4 μL) of plasma from mice in the clinical phase of mBSE (n = 4) or normal mice (n = 4) were used to seed PMCA reactions. To avoid cross-reaction to mouse immunoglobulins in the plasma, the PrP Fab D13 (epitope amino acids 96–104) was used to detect PK-digested samples. (B) Second-round reactions were seeded with 10% (8 μL) of each first-round reaction volume and analyzed as in (A). rMoPrP, 50 ng rMoPrP without PK treatment.

in plasma among different animals. Furthermore, because we observed that diluted BH frequently lost its seeding activity following freezing and thawing, especially when it contained very low concentrations of PrP^{Sc} ($< 1\ fg{\cdot}\mu L^{-1}$), freeze–thawing of the plasma may have affected the activity. Nevertheless, these results indicate that, under optimal sonication conditions, PMCA is capable of detecting PrP^{Sc} in plasma from mBSE-infected mice within a single reaction round, or two rounds at the most.

Collectively, our findings suggest that ultrasensitive detection of PrP^{Sc} is achievable by one-round PMCA, thereby greatly promoting the opportunities for the development of practical assays for TSEs including CJD and BSE.

Materials and methods

Substrate preparation for PMCA

Normal brain tissues were isolated from healthy ddY mice (8 weeks old, male), and were immediately frozen and stored at −80 °C. Frozen tissues were homogenized at 10% (w/v) in PMCA buffer (150 mM NaCl, 50 mM Hepes pH 7.0, 1% Triton X-100 and EDTA-free protease inhibitor mixture; Roche, Mannheim, Germany) using a Multi-beads-shocker (Yasui Kikai, Osaka, Japan). After centrifugation at 2000 *g* for 2 min, supernatants were collected as NBH and frozen at −80 °C until use. Total protein concentrations in NBH were determined by the BCA protein assay (Pierce, Rockford, IL, USA).

Prion strains

The origin of mBSE was as described previously [27]. mBSE and Chandler were serially passaged into ddY mice by intracerebral inoculation. Infectious titers were estimated by endpoint titration studies to be $10^{8.5}$ and $10^{7.8}$ LD_{50} units·g^{-1} of brain tissues infected with mBSE and Chandler, respectively. The brains of terminal-stage mice were collected and frozen at −80 °C until use. All animal experiments were performed in accordance with the guidelines for animal experimentation of Nagasaki University (Japan).

Seed preparation for PMCA

BHs derived from mice infected with either mBSE or Chandler strain were prepared as described above. Dilutions of the seed-BHs were carried out in PMCA buffer immediately prior to the PMCA reactions. For plasma collection, blood was collected from the hearts of normal or mBSE-infected mice using a syringe containing EDTA. Blood samples were centrifuged at 2000 *g* for 10 min, and the plasma fraction was recovered and stored frozen at −80 °C.

Dot blots

BHs and recombinant mouse PrP(23-231) were plotted on nitrocellulose membranes under mild vacuum-assisted conditions using a bio-blot (Bio-Rad, Hercules, CA, USA). Membranes were treated with 3 M guanidium thiothyanate for 10 min to denature the proteins. After washing with NaCl/Tris buffer (10 mM Tris/HCl pH 7.8, 100 mM NaCl) and blocking with 5% skimmed milk in NaCl/Tris buffer plus 0.1% Tween 20 for 60 min, membranes were probed with SAF61 anti-PrP mAb (SPI bio, Montigny le Bretonneux, France), and the immunoreactive dots were visualized using ECL-plus reagents (GE Healthcare, Piscataway, NJ, USA). Dot intensities were measured for the unit area on the membranes using LAS-3000 mini (Fujifilm, Tokyo, Japan).

Protein misfolding cyclic amplification

To avoid contamination, preparation of noninfectious material was conducted inside a biological safety cabinet in a prion-free laboratory and aerosol-resistant tips were used. Substrates (NBH; 7 mg·mL^{-1}) and seeds were prepared in 0.2 mL PCR tube strips as 80 μL solutions containing 1 mM EDTA and 0.05% digitonin, except in the experiments shown in Fig. 1 in which EDTA and digitonin were omitted as a control. Diluted mBSE- or Chandler-BH and plasma were used as seeds for the PMCA reactions. To

circumvent the influence of sample position on the delivery of vibrational energy to the samples, up to three PCR tube strips (24 samples) were placed at the same time in a floating 96-well rack in a sonicator cup horn (Model 3000 with deep-well type microplate horn; Misonix, Farmingdale, NY, USA) and immersed in 600 mL of water in the sonicator bath. The cup horn was kept in an incubator set at 40 °C during the entire PMCA reaction. Sonication was intermittently performed every 30 min at 60% power. Sonication times are described in the figure legends.

Proteinase K digestion, SDS/PAGE and western blotting

After the PMCA reactions, all samples were digested with 20 $\mu g \cdot mL^{-1}$ PK at 37 °C for 1 h. In some experiments, PNGase F (New England Biolabs, Ipswich, MA, USA) treatment was performed after PK digestion. A fourth volume of 5× SDS sample buffer (20% SDS, 10% β-mercaptoethanol, 40% glycerol, 0.1% bromophenol blue and 250 mM Tris/HCl pH 6.8) was added. Samples (final volume, 32 μL) were then boiled for 5 min, loaded onto 1.5 mm, 12 or 15% SDS polyacrylamide gels, and transferred to polyvinylidene difluoride membranes (Millipore, Billerica, MA, USA). The membranes were probed with ICSM35 (D-Gen, London, UK), SAF83 (SPI bio, Montigny le Bretonneux, France) or D13 (kindly provided by B. Caughey, Hamilton, MT, USA) anti-PrP mAbs, and visualized using Attophos AP Fluorescent Substrate system (Promega, Madison, WI, USA), in accordance with the manufacturer's recommendations.

Acknowledgements

This work was supported in part by a Grant-in-Aid for Scientific Research from the Japan Society for the Promotion of Science, Health Labor Sciences Research Grant from the Ministry of Health and Welfare of Japan, and the President's Discretionary Fund of Nagasaki University, Japan. We thank Hitoki Yamanaka and Kazunori Sano for helpful discussions and critical assessment of the manuscript, and Mari Kudo for technical assistance.

References

1 Bradley R, Collee JG & Liberski PP (2006) Variant CJD (vCJD) and bovine spongiform encephalopathy (BSE): 10 and 20 years on: part 1. *Folia Neuropathol* **44**, 93–101.
2 Collee JG, Bradley R & Liberski PP (2006) Variant CJD (vCJD) and bovine spongiform encephalopathy (BSE): 10 and 20 years on: part 2. *Folia Neuropathol* **44**, 102–110.
3 Wroe SJ, Pal S, Siddique D, Hyare H, Macfarlane R, Joiner S, Linehan JM, Brandner S, Wadsworth JD, Hewitt P *et al.* (2006) Clinical presentation and pre-mortem diagnosis of variant Creutzfeldt–Jakob disease associated with blood transfusion: a case report. *Lancet* **368**, 2061–2067.
4 Caughey B (2001) Interactions between prion protein isoforms: the kiss of death? *Trends Biochem Sci* **26**, 235–242.
5 Saborio GP, Permanne B & Soto C (2001) Sensitive detection of pathological prion protein by cyclic amplification of protein misfolding. *Nature* **411**, 810–813.
6 Castilla J, Saa P & Soto C (2005) Detection of prions in blood. *Nat Med* **11**, 982–985.
7 Gonzalez-Romero D, Barria MA, Leon P, Morales R & Soto C (2008) Detection of infectious prions in urine. *FEBS Lett* **582**, 3161–3166.
8 Murayama Y, Yoshioka M, Okada H, Takata M, Yokoyama T & Mohri S (2007) Urinary excretion and blood level of prions in scrapie-infected hamsters. *J Gen Virol* **88**, 2890–2898.
9 Saa P, Castilla J & Soto C (2006) Ultra-efficient replication of infectious prions by automated protein misfolding cyclic amplification. *J Biol Chem* **281**, 35245–35252.
10 Soto C, Anderes L, Suardi S, Cardone F, Castilla J, Frossard MJ, Peano S, Saa P, Limido L, Carbonatto M *et al.* (2005) Pre-symptomatic detection of prions by cyclic amplification of protein misfolding. *FEBS Lett* **579**, 638–642.
11 Murayama Y, Yoshioka M, Yokoyama T, Iwamaru Y, Imamura M, Masujin K, Yoshiba S & Mohri S (2007) Efficient *in vitro* amplification of a mouse-adapted scrapie prion protein. *Neurosci Lett* **413**, 270–273.
12 Kurt TD, Perrott MR, Wilusz CJ, Wilusz J, Supattapone S, Telling GC, Zabel MD & Hoover EA (2007) Efficient *in vitro* amplification of chronic wasting disease PrPRES. *J Virol* **81**, 9605–9608.
13 Jones M, Peden AH, Prowse CV, Groner A, Manson JC, Turner ML, Ironside JW, MacGregor IR & Head MW (2007) *In vitro* amplification and detection of variant Creutzfeldt–Jakob disease PrPSc. *J Pathol* **213**, 21–26.
14 Deleault NR, Harris BT, Rees JR & Supattapone S (2007) Formation of native prions from minimal components *in vitro*. *Proc Natl Acad Sci USA* **104**, 9741–9746.
15 Thorne L & Terry LA (2008) *In vitro* amplification of PrPSc derived from the brain and blood of sheep infected with scrapie. *J Gen Virol* **89**, 3177–3184.
16 Atarashi R, Moore RA, Sim VL, Hughson AG, Dorward DW, Onwubiko HA, Priola SA & Caughey B (2007) Ultrasensitive detection of scrapie prion protein using seeded conversion of recombinant prion protein. *Nat Methods* **4**, 645–650.

17 Atarashi R, Wilham JM, Christensen L, Hughson AG, Moore RA, Johnson LM, Onwubiko HA, Priola SA & Caughey B (2008) Simplified ultrasensitive prion detection by recombinant PrP conversion with shaking. *Nat Methods* **5**, 211–212.
18 Colby DW, Zhang Q, Wang S, Groth D, Legname G, Riesner D & Prusiner SB (2007) Prion detection by an amyloid seeding assay. *Proc Natl Acad Sci USA* **104**, 20914–20919.
19 Stohr J, Weinmann N, Wille H, Kaimann T, Nagel-Steger L, Birkmann E, Panza G, Prusiner SB, Eigen M & Riesner D (2008) Mechanisms of prion protein assembly into amyloid. *Proc Natl Acad Sci USA* **105**, 2409–2414.
20 Panza G, Stohr J, Dumpitak C, Papathanassiou D, Weiss J, Riesner D, Willbold D & Birkmann E (2008) Spontaneous and BSE-prion-seeded amyloid formation of full length recombinant bovine prion protein. *Biochem Biophys Res Commun* **373**, 493–497.
21 Orem NR, Geoghegan JC, Deleault NR, Kascsak R & Supattapone S (2006) Copper (II) ions potently inhibit purified PrPres amplification. *J Neurochem* **96**, 1409–1415.
22 Bocharova OV, Breydo L, Salnikov VV & Baskakov IV (2005) Copper(II) inhibits *in vitro* conversion of prion protein into amyloid fibrils. *Biochemistry* **44**, 6776–6787.
23 Yuan J, Xiao X, McGeehan J, Dong Z, Cali I, Fujioka H, Kong Q, Kneale G, Gambetti P & Zou WQ (2006) Insoluble aggregates and protease-resistant conformers of prion protein in uninfected human brains. *J Biol Chem* **281**, 34848–34858.
24 Kobayashi A, Satoh S, Ironside JW, Mohri S & Kitamoto T (2005) Type 1 and type 2 human PrPSc have different aggregation sizes in methionine homozygotes with sporadic, iatrogenic and variant Creutzfeldt–Jakob disease. *J Gen Virol* **86**, 237–240.
25 Weber P, Reznicek L, Mitteregger G, Kretzschmar H & Giese A (2008) Differential effects of prion particle size on infectivity *in vivo* and *in vitro*. *Biochem Biophys Res Commun* **369**, 924–928.
26 Silveira JR, Raymond GJ, Hughson AG, Race RE, Sim VL, Hayes SF & Caughey B (2005) The most infectious prion protein particles. *Nature* **437**, 257–261.
27 Takakura Y, Yamaguchi N, Nakagaki T, Satoh K, Kira J & Nishida N (2008) Bone marrow stroma cells are susceptible to prion infection. *Biochem Biophys Res Commun* **377**, 957–961.

European Journal of Endocrinology (2009) **161** 939–945 ISSN 0804-4643

CLINICAL STUDY

Synaptophysin immunoreactivity in adrenocortical adenomas: a correlation between synaptophysin and CYP17A1 expression

Kazuto Shigematsu, Noriyuki Nishida[1], Hideki Sakai[2], Tsukasa Igawa[2], Kan Toriyama, Akira Nakatani, Osamu Takahara and Kioko Kawai[3]

Department of Pathology, Japanese Red-Cross Nagasaki Atomic Bomb Hospital, Nagasaki 852-8511, Japan, [1]Divisions of Molecular Microbiology and Immunology, [2]Nephro-Urology, Nagasaki University Graduate School of Biomedical Sciences, Nagasaki 852-8523, Japan and [3]Department of Pathology, Nagasaki Prefecture Medical Health Operation Group, Isahaya 859-0401, Japan

(Correspondence should be addressed to K Shigematsu; Email: shigek@nagasaki-med.jrc.or.jp)

Abstract

Design and methods: The adrenal cortex is not considered to be an intrinsic part of the diffuse neuroendocrine system, but adrenocortical neoplasms possess neuroendocrine properties. In this study, we examined synaptophysin (SYP) and neural cell adhesion molecule (NCAM) expression in adrenocortical adenomas in relation to adrenal function.

Results: Immunohistochemical analysis showed that 50.7 and 98.6% of the cortical adenomas showed SYP and NCAM immunoreactivities respectively. There was no apparent difference in NCAM immunoreactivity among the adenomas. However, the immunostaining for SYP was significantly stronger in cortisol-producing adenomas (CPA) than in aldosterone-producing adenomas (APA), nonfunctioning adenomas (NFA), showing no clinical or endocrinological abnormality, or adenomas associated with preclinical Cushing's syndrome (preCS). Western blotting and real-time PCR demonstrated that the expression level of SYP protein and mRNA was significantly higher in CPA than in APA or NFA. Additionally, the SYP mRNA level showed a positive correlation with CYP17A1 mRNA. In addition to the plasma membrane, mitochondria, and smooth endoplasmic reticulum, SYP immunoreactivity was detected in the Golgi area, which is known to be involved in the regulation of mitochondrial cholesterol and the transport of steroid intermediates. It was unexpected that the ratio of positive cells for SYP in preCS was less than that in APA and NFA. However, further examination is required, because the number of preCS cases we investigated was very small.

Conclusions: We propose that SYP expression in adrenocortical cells may be involved in some aspect of adrenal function such as transport or secretion of glucocorticoids.

European Journal of Endocrinology **161** 939–945

Introduction

Hyperfunction of the adrenal cortex is associated with either hyperplasia, adenoma, or carcinoma. There are principally three forms of adrenocortical hyperfunction, namely, primary aldosteronism (PA), Cushing's syndrome (CS), and congenital adrenal hyperplasia, although extremely rare cases such as androgen- or estrogen-secreting adrenocortical tumors have been reported (1, 2). Immunohistochemistry (3–5) and *in situ* hybridization (6, 7) for steroidogenic enzymes have been attempted, as it is difficult to determine the adrenal function from the histological findings alone. However, the mechanism involved in the release of steroids from the cortical cells remains unknown, due to the absence of obvious secretory granules in the cells.

Although the adrenal cortex is not an intrinsic part of the diffuse neuroendocrine system (DNS) (8), neuroendocrine differentiation, as evidenced by immunohistochemical detection of neuroendocrine markers, is encountered in some adrenocortical tumors (9–13). An integral membrane protein, synaptophysin (SYP; molecular weight, 38-kDa) is involved in synaptic vesicle formation (14) and is well accepted as a neuroendocrine marker (15). On the other hand, the expression of the SYP gene family is not restricted to neuronal and neuroendocrine differentiation in rats or humans (16, 17). Neural cell adhesion molecule (NCAM) is a cell surface glycoprotein involved in cell–cell interactions and is thought to play a role in axonal growth and cell migration (18, 19). NCAM expression is noted not only in neuronal and neuroendocrine tissues, but also in endocrine tissues (20). In the adrenal cortex, staining for NCAM is restricted to the definitive zone (DZ) in the fetus and the zona glomerulosa (ZG) in adults, both of which express aldosterone synthase (12, 21). Although two large NCAM protein isoforms, with apparent molecular masses of 180- and 140-kDa, have been characterized, the 180-kDa isoform is more common in neuronal tissues and the 140-kDa isoform has been

DOI: 10.1530/EJE-09-0596
Online version via www.eje-online.org

noted in endocrine tissues (20). Hence, it is possible that NCAM may play a different role in neuronal and endocrine tissues.

These observations led us to the suggestion that both SYP and NCAM may be involved in some aspect of adrenal function. In this study, we examined the expression of SYP and NCAM in association with endocrine function in adrenocortical adenomas by using immunohistochemistry, western blotting, and real-time PCR.

Materials and methods

Tissue samples

Of the human adrenal tissues listed in Nagasaki University Graduate School of Biomedical Sciences between 2001 and 2008, 29 cases of aldosterone-producing adenomas (APA), 20 cases of cortisol-producing adenomas (CPA), two cases of APA with CS, two cases of APA with preclinical CS (preCS), two cases of adenomas associated with preCS, and 16 cases of clinically silent nonfunctioning adenomas (NFA) were identified (see Supplementary Table 1, which can be viewed online at http://www.eje-online.org/supplemental/). The plasma aldosterone concentration (PAC)/plasma renin activity (PRA) ratio ($\geq$25) was used in screening for PA. Subsequently, PA was diagnosed on the basis of an elevated PAC and suppressed PRA. The diagnosis of CS was based on specific clinical symptoms such as obesity, moon face, buffalo hump, abdominal striae, etc. elevated plasma cortisol concentration with lack of diurnal rhythm; and a suppressed plasma ACTH level. A diagnosis of preCS was made on the basis of: a) the presence of adrenal incidentaloma with lack of specific clinical symptoms of CS, b) abnormal circadian rhythm (normal plasma cortisol levels at early morning and elevated plasma cortisol levels at late evening), c) demonstration of autonomous secretion of cortisol by the overnight mg dexamethasone suppression test, d) inhibition of ACTH secretion, e) postoperative adrenal insufficiency or atrophy of the attached adrenal cortex, etc. Clinically silent adrenal incidentalomas showing no signs of PA, CS, or preCS were classified as NFA. Imaging of the adrenal glands with computerized tomography and scintigraphy was done for detection of adrenal masses. Furthermore, all patients were examined by adrenal venous sampling to determine the aldosterone-to-cortisol ratio on the right and left sides. Adrenocortical adenomas were diagnosed according to the histopathologic criteria proposed by Weiss *et al.* (22, 23). As controls, we used adrenal glands obtained from patients undergoing adrenalectomy together with pancreatectomy or nephrectomy for pancreatic or renal cancer, who did not reveal any endocrine abnormalities.

Immunohistochemistry

Paraffin-embedded tissues were cut on a microtome to a thickness of 4 μm. After deparaffinization, heat-induced epitope retrieval with Dako target retrieval solution (pH 6.0; DakoCytomation, Kyoto, Japan) was performed. The tissue sections were allowed to react overnight at 4 °C with anti-SYP (SY38 clone, dilution 1/20; Dako), anti-NCAM (123C3 clone, dilution 1/20; Zymed Corp., South San Francisco, CA, USA), or anti-Golgi apparatus protein 1 precursor (GLG1; dilution 1/75; Sigma–Aldrich) antibodies. Double staining with SYP and GLG1 was also performed using the HISTOSTAIN-DS KIT (Zymed). For determination of antibody specificity, immunostaining was prevented by preincubation of anti-SYP antibody with an excess of recombinant human SYP (Thermo Fisher Scientific, Fremont, CA, USA), and nonimmune mouse or rabbit sera were substituted for anti-NCAM or GLG1 antibodies respectively. The data obtained were expressed as scores ranging from 1 (<10% positive cells) to 2 (10–30% positive cells), to 3 (30–50% positive cells), and to 4 (50–100% positive cells). In cases with no reaction, a score of 0 was recorded.

Western blotting

Five cases of APA and seven cases of CPA were used for the detection of SYP and NCAM proteins by western blotting. Frozen adenoma tissues were homogenized on ice for 1 min in lysis buffer containing protease inhibitor cocktail (Nakarai, Kyoto, Japan). To obtain detailed information on the subcellular distribution of SYP immunoreactivity, homogenates of adrenal tissues were also fractionated into mitochondria, microsome derived from fragmented smooth endoplasmic reticulum (sER), and plasma membrane, as described previously (24). The protein extracts (40 μg each) were subjected to SDS-12% PAGE. After the proteins were transferred onto an Immobilon-P membrane (Nihon Millipore Ltd, Tokyo, Japan), the membrane was reacted with anti-SYP (dilution 1/50; Dako) or anti-NCAM (dilution 1/50; Zymed) for 1 h at room temperature. The optical densities were measured by NIH image and were standardized by β-actin.

Real-time PCR

To examine the expression of SYP, 140-kDa NCAM, CYP11B2, and CYP17A1 mRNAs, we performed real-time PCR amplification in seven cases of APA, 13 cases of CPA, and four cases of NFA. Total RNA was collected from frozen adenoma tissues using GenElute Mammalian Total RNA kit (Sigma–Aldrich). After the reverse transcriptase reaction, LightCycler Quick System 330 (Roche Diagnostics K K) was used for the real-time PCR (7). Sequence-specific primers were designed and assigned the following GenBank accession

numbers: SYP (X06389: 225–249 and 357–333), 140-kDa NCAM (M17410: 919–937 and 993–972), CYP11B2 (X54741: 2637–2658 and 2724–2699), and CYP17A1 (M14564: 1203–1226 and 1339–1315). Expression levels were standardized by 18S rRNA (M10098: 124–148 and 256–232). All products were checked by electrophoresis using 3% agarose gels and ethidium bromide staining with u.v. visualization to ensure the specificity of the PCR products and the absence of nonspecific bands. Relative quantitation of gene expression was performed using the relative standard curve method.

Ethics

All patients signed a form of informed consent prepared in accordance with the rules outlined by the Nagasaki University Ethics Committee.

Statistical analysis

Differences were analyzed with Spearman's correlation coefficient by rank test, Student's *t*-test, Pearson's correlation coefficient test, and χ^2 for independent test. Results were expressed as the mean ± S.E.M.

Results

In the control adrenal cortices, immunoreactivity for SYP was present in the nerve fibers, appearing as small dots, while NCAM immunostaining was present in the ZG and outer zona fasciculata (ZF) (data not shown). In the adenomas, SYP immunoreactivity was detected along the plasma and lipid membranes (Fig. 1a), and cytoplasm. Immunoreactivity manifesting as large dots was also observed in the perinuclear Golgi area, which well accorded with the localization of GLG1 staining (Fig. 1b). The immunoreaction for NCAM was limited to the plasma membrane (Fig. 1c). There was no evidence of positive immunostaining in the negative control sections (Fig. 1d).

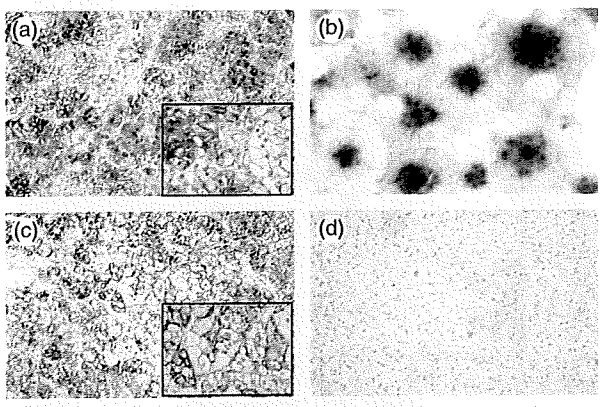

Figure 1 Immunohistochemical staining for SYP and NCAM with hematoxylin counterstaining in adrenocortical adenomas. Immunoreactivity of SYP is located along the plasma and lipid membranes. (a) SYP staining is also present in the perinuclear Golgi area. Double staining for SYP (red color) and GLG1 (blue color) indicates that SYP and GLG1 are colocalized in the Golgi area. (b) The immunoreaction for NCAM was limited to the plasma membrane (c). In (d), a negative control is indicated. (a), (c) and (d), ×100; (b), ×400; squares in (a) and (c), ×200.

Table 1 Immunoreactivity for synaptophysin in adrenocortical adenomas.

	0+	1+	2+	3+	4+	Total
APA	16	12	0	1	0	29
CPA	0	0	0	4	16	20
PA+preCS	2	0	0	0	0	2
PA+CS	0	0	1	1	0	2
preCS	2	0	0	0	0	2
NFA	15	0	1	0	0	16

Staining score: 1+, <10%; 2+, 10–30%; 3+, 30–50%; 4+, >50%. Intensity of staining: CPA>PA+CS>APA=NFA>PA+preCS=preCS ($P<0.01$).

The results of staining for SYP and NCAM are summarized in Tables 1 and 2. Of the 71 cases of adrenocortical adenomas, 36 (50.7%) and 70 (98.6%) showed SYP and NCAM immunoreactivities respectively, although the component cells of adenomas were not all positive for SYP or NCAM. With the exception of one case where a staining score 3 was recorded, the APA showed only a faint (staining score 1) or no SYP immunoreactivity. All cases of preCS (containing APA with preCS) and 15 out of 16 cases of NFA also showed no SYP immunoreactivity. On the other hand, intense staining of SYP was observed in all cases of CPA (staining score 3–4). The intensity of staining for SYP was significantly stronger in the adrenocortical adenomas associated with overt CS than in the adenomas not associated with overt CS (Spearman's correlation coefficient by rank test, $P<0.01$). Unexpectedly, the intensity of SYP immunoreactivity in preCS was less than that in APA and NFA. A significant relationship between the intensity of staining for NCAM and clinical symptoms was not observed, although there was a tendency to intensely stain among the APA.

Western blotting demonstrated a 38-kDa SYP band in the control adrenal gland (containing adrenal medulla) and all cases of CPA, but not in the APA cases (Fig. 2a). Immunoreactivity was present in all the subcellular

Table 2 Immunoreactivity for neural cell adhesion molecule in adrenocortical adenomas.

	0+	1+	2+	3+	4+	Total
APA	0	0	0	2	27	29
CPA	0	1	5	6	8	20
PA+preCS	0	0	0	1	1	2
PA+CS	0	0	0	0	2	2
preCS	0	0	1	1	0	2
NFA	1	1	4	4	6	16

Staining score: 1+, <10%; 2+, 10–30%; 3+, 30–50%; 4+, >50%. Intensity of staining: no significant difference was observed.

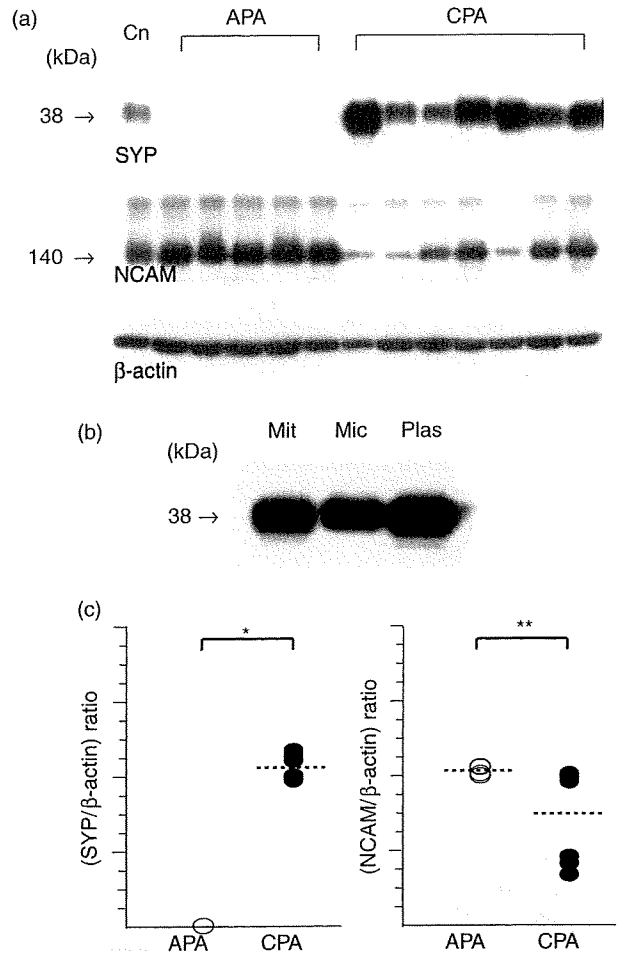

Figure 2 Western blot analysis. A 38-kDa SYP band is detected in the control adrenal and all cases of CPA, but not in APA (a, upper panel; c, left panel). SYP immunoreactivity was present in the fractions of mitochondria (Mit), microsome (Mic), and plasma membrane (Plas) (b). All cases demonstrate 140-kDa NCAM band (a, middle panel), but the optical density of the band standardized by β-actin (a, lower panel) is slightly higher in APA than in CPA (c, right panel). Dotted lines show the mean value in APA and CPA tissues respectively. *$P<0.01$, **$P<0.05$. Cn, control adrenal (containing the medulla).

fractions of mitochondria, microsome, and plasma membrane (Fig. 2b). Meanwhile, all cases examined showed mainly a 140-kDa band reacting with MAB against NCAM (Fig. 2a), and the optical density of the band was slightly higher in APA ($n=5$; 1.06 ± 0.03) than in CPA ($n=7$; 0.76 ± 0.11) (Student's t-test, $P<0.05$; Fig. 2c).

Real-time PCR (Fig. 3a) demonstrated that the expression level of SYP mRNA was about tenfold higher in CPA ($n=13$; $1.20\pm0.12\times10^{-4}$) than in APA ($n=7$; $0.10\pm0.03\times10^{-4}$) and NFA ($n=4$; $0.11\pm0.05\times10^{-4}$) (Student's t-test, $P<0.001$). On the other hand, 140-kDa NCAM mRNA was more highly expressed in APA ($n=7$; $0.97\pm0.05\times10^{-6}$) and NFA ($n=4$; $1.05\pm0.08\times10^{-6}$) than in CPA ($n=13$; $0.80\pm0.03\times10^{-6}$; $P<0.05$). To determine whether or not the expression of SYP or NCAM mRNA correlated with steroidogenesis, we also examined the expression of CYP11B2 and CYP17A1 mRNAs, encoding aldosterone synthase, the enzyme for the final step of aldosterone synthesis, and 17α-hydroxylase (17α-OH), the limiting enzyme in cortisol synthesis respectively. As expected, high levels of CYP11B2 and CYP17A1 mRNAs were observed in APA and CPA respectively (data not shown). High expression of CYP17A1 mRNA in CPA was also confirmed by *in situ* hybridization (see Supplementary Table 2, which can be viewed online at http://www.eje-online.org/supplemental/). The expression level of SYP mRNA correlated positively with that of CYP17A1 mRNA (Pearson's correlation coefficient test, $n=24$; $r=0.8532$, $P<0.001$; Fig. 3b). No significant correlation was found between NCAM mRNA and endocrine function.

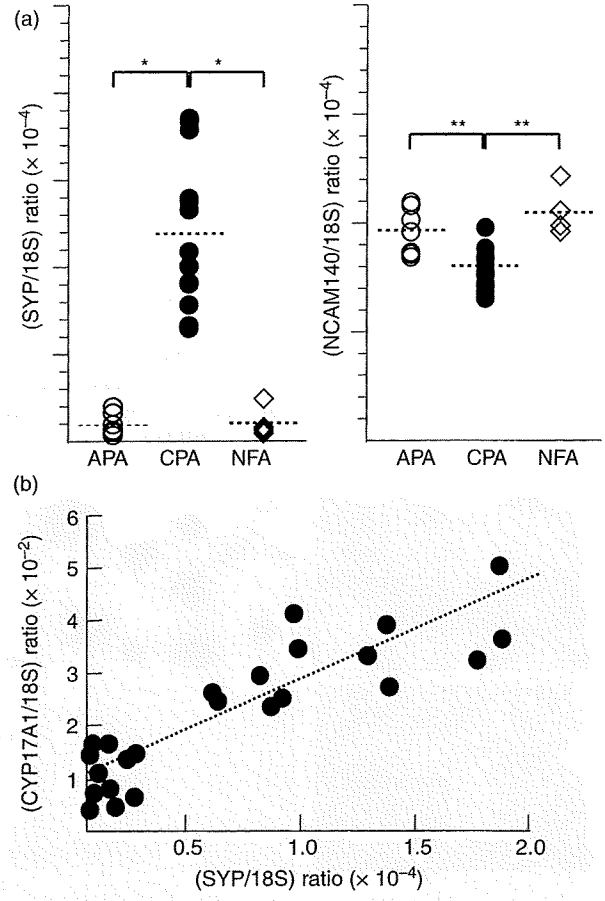

Figure 3 Analysis of SYP, 140-kDa NCAM and CYP17A1 mRNA expression by real-time PCR. (a) The results are shown as the ratio of SYP (left panel) and 140-kDa NCAM (right panel) to 18S rRNA. Dotted lines show the mean value in APA, CPA, and NFA tissues respectively. *$P<0.01$, **$P<0.05$. (b) A correlation between SYP and CYP17A1 mRNA expression. The expression level of SYP mRNA shows a positive correlation with CYP17A1 mRNA ($P<0.01$).

Discussion

Previous studies (9–13) reported that SYP and NCAM were ubiquitously expressed in adrenocortical tumors, but detailed examination of the differences in the expression among adrenal disorders has not been extensively performed. In this study, we examined SYP and NCAM expression in adrenocortical tumors using immunohistochemistry, in relation to adrenal function. The specificity of the immunoreactivities was confirmed by a preabsorption test or by substitution of nonimmune mouse sera in place of the primary antibodies. Western blotting, using the same antibodies as in the immunohistochemistry, also demonstrated a specific band: 38-kDa in SYP (12, 14) and 140-kDa in NCAM (12). Hence, the immunostaining in this study was specific with no false positives.

The implication of the finding that adrenocortical adenomas exhibit neuroendocrine properties such as SYP and NCAM, despite the fact that the adrenal cortex is not an intrinsic part of the DNS, is as yet little understood (8). Haak *et al.* (10) suggested the possibility that the staining cells might be derived from remnants of the fetal adrenal cortex and that silent genes might emerge under physiological conditions, as a result of dedifferentiation of adrenocortical cells. The DZ cells in the human fetal cortex are thought to be a progenitor (stem) population, capable of migrating into other zones (21). Aldosterone synthase and other steroidogenic enzymes are expressed at late gestation by DZ cells, like ZG cells in the adult adrenal (10, 25). Additionally, as NCAM protein and mRNA are expressed in DZ cells as well as ZG cells (12, 21), this hypothesis could explain why NCAM expression was present in most of the adenomas, especially APA. However, the hypothesis fails to account for the significant difference in SYP expression among the adenomas. In this study, CPA exhibited a high ratio of positive cells for SYP, whereas APA, the adenomas associated with preCS, and NFA showed few positive cells. Our result differed from the report of Li *et al.* that there seemed to be no correlation between SYP expression and endocrine clinical syndrome (13). However, our findings were supported by the results of western blotting and real-time PCR, demonstrating that the expression level of SYP protein and mRNA was significantly higher in CPA than in APA or NFA. In general, a nonspecific- or over-staining sometimes appears, depending on the antibody (especially polyclonal antibody), in the kidney and adrenal gland. Li *et al.* used a SYP polyclonal antibody in addition to monoclonal (13), whereas we used only monoclonal to avoid nonspecific binding as much as possible. Therefore, the type of antibody used may account for the differing results.

SYP is one of the major polypeptide components of the small electron-translucent vesicles of neurons and DNS cells (14, 16), and its presence in endocrine tumors correlates with the presence of cytoplasmic dense core granules (26). Furthermore, SYP is thought to contribute fundamentally to controls of the exocytotic process in non-DNS cells, such as thymic epithelial cells (16, 17). In adrenal glands, the biosynthetic steps involved in steroidogenesis are well elucidated (4, 27), but the secretory mechanism involved in the release of steroids from the adrenocortical cells is little understood, because the intracellular localization of the steroids is obscure. In addition to the plasma membrane, SYP immunostaining was present in the cytoplasm. Western blotting using subcellular fractions indicated that the immunoreactivity was localized in fractions containing mitochondria and microsome deriving from fragmented sER expressing the P450 enzymes necessary for steroid hormone production (27). Additionally, we demonstrated in this study that the SYP mRNA level showed a positive correlation with the mRNA level of CYP17A1 encoding 17α-OH, but not CYP11B2 mRNA encoding aldosterone synthase. Furthermore, of particular interest is the observation that the staining for SYP was detected in the Golgi area, as proved by GLG1 staining. The Golgi apparatus in the adrenal cortex has been thought to be involved in the regulation of mitochondrial cholesterol, the transport of steroid intermediates, and the regulation of plasma and lysosomal proteins (28, 29). Bassett & Pollard (30) reported that Golgi-related coated vesicles in rat ZF cells might be related to the transport of corticosterone (corresponding to cortisol in human) to the plasma membrane, based on the correlation between the vesicle numbers and plasma corticosterone concentration. Similar vesicle-like structures have been reported to be present also in human adrenocortical tumors and in primary pigmented nodular adrenocortical disease (9, 31, 32). The data thus far collectively imply that SYP expression may be involved in adrenal function, such as in the transport or secretion of glucocorticoids.

The expression level of SYP may be dependent upon the amount of steroid production in each cell. This would also explain why SYP was undetectable in adenomas associated with preCS. Additionally, it was no surprise to find heterogeneity of SYP staining in the same adrenal tumor, because the component cells of tumors do not all consistently synthesize or secrete steroid hormones at the same level. However, it was unexpected that the intensity for SYP staining in preCS was weaker than that in APA or NFA. Further examination is required to confirm whether there is actually any difference among APA, NFA, and preCS, because the number of preCS cases we investigated was very small. On the other hand, the real-time PCR showed that APA and NFA expressed SYP mRNA at the same, albeit very low, level, which is consistent with the fact that both APA and NFA have the potential for cortisol synthesis within the normal range (33).

Although we found no evidence of any relationship between NCAM and adrenal function, the results of immunohistochemistry, western blotting, and real-time